Composites: Part A 182 (2024) 108211

Contents lists available at ScienceDirect

Composites Part A

journal homepage: www.elsevier.com/locate/compositesa

Manufacturing of thermoplastic composite sandwich panels using induction welding under vacuum

R.G. Martin [a], C. Johansson [b], J.R. Tavares [c], M. Dubé [a,*]

[a] CREPEC, Mechanical Engineering, École de Technologie Supérieure, Montréal, Canada
[b] RISE Research Institutes of Sweden, Göteborg, Sweden
[c] CREPEC, Chemical Engineering, Polytechnique Montréal, Montréal, Canada

ARTICLE INFO

Keywords:
A. Material: Honeycomb
Polymer-matrix composites (PMCs)
Sandwich structures
D. Testing: Mechanical testing
Optical microscopy
E. Manufacturing / Processing: 3-D printing
Joints/joining

ABSTRACT

A new method to manufacture thermoplastic composite sandwich panels is presented, making use of the induction welding process in which a magnetic susceptor generates the heat at the core/facesheet interface. This technique proposes a fast way to assemble thermoplastic sandwich structures without risking the deconsolidation of the composites skin. The welding pressure is obtained by applying vacuum over the sandwich panel. This vacuum induction welding method (Vac-IW) allows joining thermoplastic composite facesheets to a thermoplastic polymer core in a clean and non-contact manner. The feasibility of the method is demonstrated by preparing sandwich samples made of glass fibre reinforced polyetheretherketone (PEEK) skins and a 3D-printed polyetherimide (PEI) honeycomb core. A susceptor made of PEI and μm-sized nickel (Ni) particles is used to generate heat by magnetic hysteresis losses. The strength of the sandwich samples assembled by the Vac-IW method is evaluated by flatwise tensile (FWT) tests.

1. Introduction

The demand for thermoplastic composites in various industries, such as the aerospace and automotive sectors, has been growing in the last decades. To reduce fuel consumption and CO_2 emissions, manufacturers try to reduce the structural weight by replacing traditional materials like metals for materials exhibiting similar mechanical properties with a lower density, such as fibre reinforced composites. In the space industry, the weight is even more critical because of the high impact it has on the launch cost. Space structures must also comply with other requirements such as vibration absorption and thermal insulation to survive launch and thermal cycles faced during the mission [1]. For these purposes, sandwich panels are often selected as the main parts of the space structures.

1.1. Sandwich structures

Sandwich structures consist of two thin high-strength, high in-plane stiffness outer layers – known as facesheets or skins – and a core material located between the two skins. The low-density core provides the compression strength, supports the through-the-thickness shear loads, and contributes to the high flexural stiffness of the sandwich panel ([2–4]). These structures are lightweight and may offer shock and vibration absorption, as well as good impact resistance properties ([5,6]).

Thermoset-based sandwich panels are well-established, but their production is labour and time-intensive, and they do not fulfill current growing requirements for sustainability [7]. High-performance thermoplastic polymers and composite materials present an alternative in sandwich structures, as they offer an ideal combination of light weight, thermal stability and high mechanical properties making them ideal candidates for aerospace and automotive structures [7]. Many thermoplastic polymers are also known for their high fracture toughness, good chemical stability and unlimited shelf life [5]. They also offer a high potential of being recycled [8].

There are different types of cores and skins commonly used in the aerospace industry. Foam cores made of materials such as polyethylene terephthalate (PET), polypropylene (PP), and polyvinyl chloride (PVC) are often retained, mostly for their compression strength, impact absorption properties and thermal insulation. Honeycomb cores made of aramid fibres or aluminium are also common due to their high strength-to-weight ratio and excellent energy absorption capability [9]. Honeycomb cores can also be made out of thermoplastic polymers, typically by joining small tubes of polymer together [10]. In recent years, additive manufacturing (or 3D-printing) has been used to produce thermoplastic

* Corresponding author.
E-mail address: martine.dube@etsmtl.ca (M. Dubé).

https://doi.org/10.1016/j.compositesa.2024.108211
Received 1 February 2024; Received in revised form 27 March 2024; Accepted 14 April 2024
Available online 15 April 2024

honeycomb cores. This process allows to create honeycomb cells with exotic shapes, like for example reentrant cells [11], with variable geometry across the thickness [12] or cores with variable in-plane density.

The skins are typically made of high-performance composite materials, such as carbon fibre reinforced polymers (CFRP) and glass fibre reinforced polymers (GFRP) [7]. The core and the skins are joined to ensure proper loads transfer through the structure. Adhesive bonding is the predominant technique used for that joining step. Although it is well-established in the aerospace industry, adhesive bonding presents limitations. Adhesives typically have a different coefficient of thermal expansion (CTE) than the bonded parts, which can lead to failure when experiencing large thermal cycles. Most of them also do not meet the space requirements with regards to outgassing, making them unusable for space applications [13].

Thermoplastic composite sandwich panels are not common. Only a few research groups have looked at the manufacturing of these structures, with an increasing interest in the recent years ([5,14–19]). Two main methods for joining the skins to the core have been reported: adhesive bonding and welding, also known as fusion bonding. Adhesive bonding is typically achieved using epoxy polymers, which present compatibility challenges with thermoplastics, and requires extensive surface preparation. The curing of the epoxy adhesives also requires time and is labour-intensive [20]. Thermoplastic welding, on the other hand, requires low to no surface preparation and is a fast process ([21,22]).

1.2. Skin-core assembly by thermoplastic welding

The joining of thermoplastic composite sandwich panels is done in a one-step or two-step process in [5]. The one-step process, referred to by the authors in [5] as “isothermal”, consists in placing the core and the two skins together in a hot press or oven and apply heat and pressure to join the skins to the core. The two-step process, referred to as “non-isothermal”, consists in heating up one face of each skin and then transferring the skins rapidly over the core and applying pressure. This second process has the advantage of not melting the core through its thickness, which may lead to collapse due to the core losing its mechanical properties past its melting temperature [23]. The pressure can be applied on the parts by placing them in a vacuum bag. Once the vacuum is pulled inside the bag, a homogeneous atmospheric pressure is applied on the sample. In such a case, the important parameters controlling the skins to core joining quality are the skins pre-heat temperature and the transfer time in the vacuum bag ([18,24]). The heat losses during transfer imply to overheat the skins in the pre-heat phase, which can lead to deconsolidation of the laminates or degradation of the polymer, therefore limiting the use of this method.

Pressure can also be applied using a hot press ([25–27]) which can reach much higher pressures than the atmospheric pressure and can also heat up the parts. This method showed some good results but faces the same challenges and limitations as vacuum moulding when a one-step process is considered with the melting of the core and associated loss of stiffness and strength. The main advantage is a shorter transfer time when a two-step process is considered, due to the possible automatization of the process. Finally, double-belt lamination is a continuous process in which parts are assembled, then guided through heating elements by two belts ([28,29]). The heat is brought to the joining interface by conduction through the skins. The parts temperature must be continuously monitored to avoid core crushing.

In all of the described techniques, the heat source is located outside of the sandwich structure and the skins are heated through their thickness. Localising the heat dissipation at the joining interface, e.g., using a welding technique, is an interesting avenue to explore for the manufacturing of thermoplastic composite sandwich panels.

2. Theoretical background

2.1. Thermoplastic welding

In practice, thermoplastic welding techniques can be divided into three mains methods: thermal welding, friction welding and electromagnetic welding [22]. Thermal welding methods consist in preheating the parts directly before assembling them under pressure. Friction welding implies that heat at the joining interface is generated due to the relative movement of the parts against each other. Electromagnetic welding is more adapted to the geometry of sandwich panels. The working principle is to place at the joining interface a material able to react to an applied electromagnetic solicitation and dissipate heat in the surrounding parts ([30–33]). When placed between the skin and the core, this material allows for welding to occur, without having to heat up the rest of the sandwich structures, preventing the risks of core crushing and skin deconsolidation, as experienced in the previously mentioned methods. The most used electromagnetic welding techniques are resistance and induction welding. Resistance welding is limited in welding width due to current leakage issues and potentially non-uniform temperature distribution [34]. It also involves connecting a heating element to a power supply which may prove difficult to scale-up and apply to a sandwich panel. This study focuses on the induction welding method.

2.2. Induction welding

Induction welding is of particular interest to the aerospace industry due to its speed and adaptability to complex geometries. It relies on the transformation of a time-varying magnetic field into heat by a heating element called a susceptor ([30,33,35,36]). Direct heating (Joule heating) of carbon fibre-based composites is possible when eddy currents are induced directly in the adherents, which is known as susceptor-less welding, as shown in Fig. 1a ([37–40]). However, a susceptor is required when direct heating is undesirable or if a non-electrically conductive composite material is used, such as glass fibre reinforced polymers. There are two main heat dissipation mechanisms happening in susceptor materials: Joule heating by eddy currents and magnetic hysteresis-losses. When subjected to a time-varying magnetic field, eddy currents are induced in electrically conductive materials, which generates heat through resistive heating, also known as Joule heating (Fig. 1b). The heating element can be a conductive mesh – such as stainless steel – or a carbon fibre woven ply [41]. It can also be a single layer of conductive polymer ([42,43]). On the other hand, susceptors based on magnetic hysteresis exploit the capability of ferromagnetic materials to absorb energy from an applied alternating magnetic field and release it into heat, inducing an increase in temperature (Fig. 1c). These susceptors are typically made of ferromagnetic micro- or nano-particles dispersed in a thermoplastic polymer (typically the same as the parts to be welded) ([44–48]). Hysteresis losses susceptors present multiple advantages. First, as there is no need to reach a percolation threshold (unlike for electrically-conductive susceptors), the particles concentration is low and impacts the mechanical properties and the weight of the susceptor to a lesser degree. As magnetic materials lose their properties – and their ability to heat up during induction welding – when passing a certain temperature known as the Curie temperature [49], it is therefore possible to get a susceptor that will not overheat [48]. This offers the opportunity to include an inherent temperature-control feature in the susceptor.

2.3. Dual-polymer bonding on sandwich skins

One major challenge when using thermoplastic welding to assemble sandwich structures is to generate enough heat at the interface to weld the parts together, while avoiding deconsolidating the skins. Grünewald et al. proposed to apply the dual-polymer bonding technique on sandwich skins to solve this issue [26].

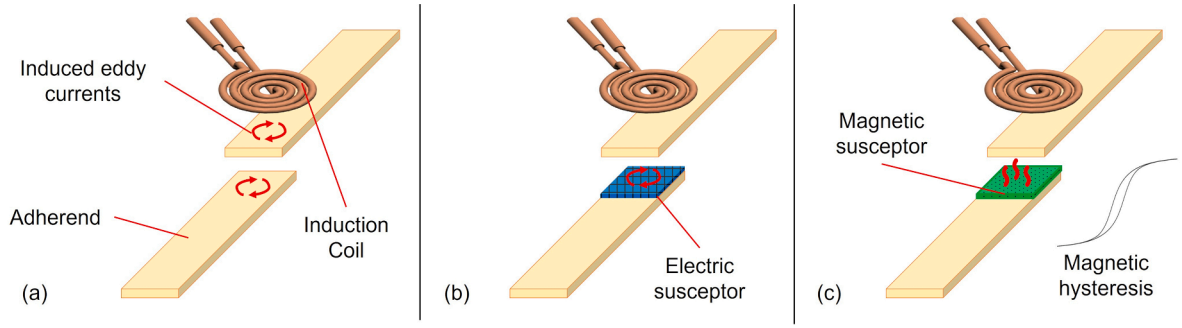

Fig. 1. Heating mechanisms in induction welding: (a) Susceptor-less welding, (b) electrically-conductive susceptor, (c) hysteresis-losses susceptor (adapted from [47]).

The dual-polymer bonding technique – or Thermabond process – consists in co-consolidating a secondary polymer on the surface of the parent laminate to be welded ([50–52]). The secondary polymer must have a processing temperature lower than that of the matrix of the parent adherend and be miscible in it. A film of the secondary polymer is added to the plies stack before consolidation. During compression moulding, the two polymers can diffuse into each other, ensuring a strong interface between them and leaving a polymer-rich layer at the surface composed of the secondary polymer. For example, it is possible to co-consolidate a polyetherimide (PEI) film on the surface of a polyetheretherketone (PEEK) adherend, as the two polymers are miscible. PEI is an amorphous thermoplastic exhibiting a glass transition temperature of 215–217 °C ([53,54]). Welding can therefore occur at a lower temperature than the melting point of PEEK (341–344 °C ([47,54])), as the joining interface is made of PEI. The authors of the original study determined a temperature range between 260 °C and 315 °C to weld PEEK adherends with co-consolidated PEI surface layers ([51,55]). By staying in that temperature range, the PEEK matrix of the skins does not melt, ensuring a better dimensional stability of the final part.

2.4. Vacuum induction welding technique

Herein, an innovative method to assemble skins to core in sandwich structures is introduced. This method uses a vacuum bag for pressure application and relies on induction to generate heat directly at the joining interface. A susceptor material based on magnetic hysteresis losses is located at the interface between the skin and the core to localize heat dissipation. As heat is generated at the same time as the pressure is applied, this method can be considered as a "one-step" process, but as the heat is generated locally and not throughout the whole structure, it is considered a welding process, contrarily to the original vacuum moulding method.

A secondary polymer with a lower welding temperature is added on the surface of the sandwich skins. This prevents the risk of laminate deconsolidation and the loss of mechanical properties of the skin. The honeycomb core exhibits low thermal conductivity, which means that the heat dissipated at the interface will not be rapidly transferred to the rest of the structure, lowering the risk of core crushing. During this process, the second skin, located on the other face of the sandwich panel, is far away from the coil. Typically, sandwich cores are half an inch to one inch thick, sometimes even more. Therefore, the opposite skin is subjected to a very low magnetic field amplitude which does not induce significant heating. This lack of direct heating and the poor heat transfer occurring by conduction through the core thickness ensure that the opposite skin is not affected by the ongoing welding process.

Therefore, the goal of this paper is to demonstrate the feasibility of the vacuum induction welding (Vac-IW) method using a hysteresis losses susceptor. First, a magnetic susceptor for the induction welding of thermoplastic composites sandwich panels is developed. Following the susceptor development, an experimental setup allowing induction welding under vacuum pressure is presented. Finally, sandwich samples are welded and characterized by optical microscopy and mechanical testing to verify the feasibility of the method.

3. Materials and methodology

3.1. Parts preparation

Honeycomb core samples are produced by Fused Filament Fabrication (FFF) additive manufacturing using an AON3D M2 3D-printer. The core is composed of 4 mm wide hexagonal cells with wall thickness of 0.8 mm and a height of 10 mm, as presented in Fig. 2. The cell dimension is selected to obtain an integral number of cells along the width of the sample (50 mm), ensuring the symmetry of the honeycomb core. The core is directly printed on the bottom sandwich skin, a 1 mm PEI layer, for a total thickness of 11 mm. A 0.8 mm thick frame wall surrounds the honeycomb core, ensuring the outer dimensions of 50 x 50 mm. ThermaX ULTEM 1010 (PEI) filament (3DxTech) is used as the feeding material and the printing parameters are the following: nozzle temperature of 390 °C, bed temperature of 160 °C and chamber temperature of 125 °C.

The top sandwich skin is made of glass fibre reinforced PEEK (GF/PEEK), with a co-consolidated 125 μm-thick PEI film (ULTEM 1000, Sabic). Glass fibre reinforcement was selected to avoid direct heating in the skin, which would happen in carbon fibres. This allows to perform the weld using a hysteresis losses susceptor and validate its use for induction welding of sandwich structures. The laminates are produced using a hot press (700 kN hot press from Pinette PEI) following a consolidation cycle of 20 min at 380 °C under a pressure of 2 MPa. To guarantee the presence of a PEI-rich surface layer at the joining interface and to avoid polymer squeezing out of the tool, a 100 μm-thick polyimide film (Kapton) is placed around the PEI film. The resulting laminates are cut into 50 mm x 50 mm samples to be used as sandwich top skins.

To prepare the susceptor film, ULTEM 1010 pellets (Sabic) and Ni particles (Sigma-Aldrich, mean diameter 5 μm) are mixed in an internal mixer at 320 °C for 5 min, with a Ni volume fraction of 10 %vol. Both materials are dried for 4 h at 150 °C beforehand to remove moisture. After mixing, the material is processed into thin films in a hot press at 320 °C. The resulting films are approximately 0.6 mm thick. Square 50 mm x 50 mm samples are cut to be used as induction welding susceptors in the sandwich panels.

The selection of Ni particles to produce a hysteresis losses susceptor for induction welding made of PEI is based on the heating properties of the particles. Compared to other magnetic materials such as magnetite or iron, Ni provides the largest heating rate at the magnetic field amplitude available with the experimental setup ([48,54]). Also, due to its Curie temperature (358 °C) close to the melting point of PEEK (343 °C), Ni cannot overheat and locally degrade the polymer during the

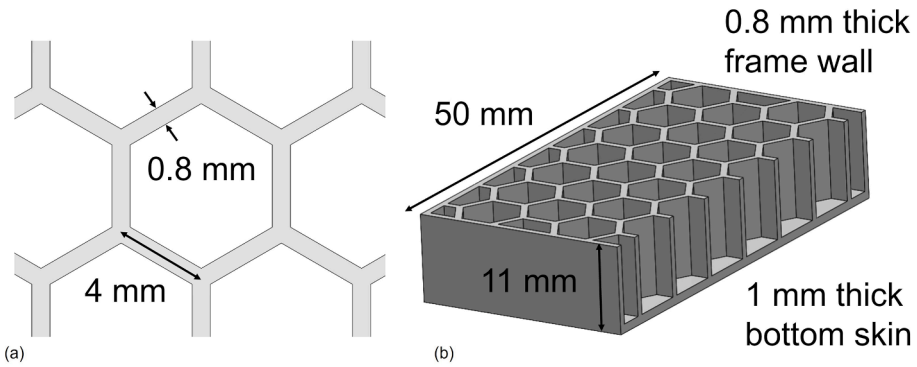

Fig. 2. (a) Schematic of the honeycomb core with the single hexagonal cell dimensions and (b) the general sample dimensions.

process. This thermal control feature makes Ni an ideal candidate for this study.

3.2. Induction welding setup

The samples are welded using a Vac-IW lab-scale setup. An Ambrell EASYHeat 10 kW generator (maximum current 750 A, frequency range 150–400 kHz) is used to produce the alternating current to the coil system. The current travels in a water-cooled copper induction coil, generating the alternating magnetic field required to perform induction welding. The frequency of the alternating current is automatically calculated by the generator, based on the coil geometry. In this case, it is fixed at 389 kHz. To increase the magnetic field amplitude in the region of the weld, a magnetic field concentrator (Ferrotron 559H from Fluxtrol) in placed around the induction coil. This low magnetic permeability material (relative magnetic permeability around 16) concentrates the magnetic field lines towards the side of the coil where the sample is located [54].

The sandwich parts to be welded are placed on a plate and covered with a vacuum bag, fixed to the plate with sealing joint. The vacuum bag is made of Kapton to sustain the high welding temperature. Once the parts are in place, vacuum is pulled, and pressure is applied on the sample during the complete duration of the Vac-IW process. Fig. 3 presents a schematic view of the Vac-IW setup used to weld the sandwich samples.

To allow for relative displacement between the sample and the induction coil, the setup is equipped with a linear displacement table enabling lateral displacement at controlled speed. The vacuum bag containing the sample to be welded is placed on this table and the distance between the sample and the induction coil is fixed. Typically, the pressure inside the bag reaches −90 kPa and is maintained during the process.

A total of 17 samples are prepared to evaluate the welding interface and for mechanical characterization. The different parts of the sandwich panels are simply wiped with alcohol before assembly to remove dust. No other surface preparation is performed before welding.

The influence of the welding speed, or the relative speed between the induction coil and the sample, is evaluated in this study. It has been reported in the literature that changing the welding speed during continuous induction welding process affects the thermal history at the weld line [56]. The alternating current amplitude is fixed at 600 A, the frequency at 389 kHz, and the coupling distance at 3 mm for all samples. Based on previous work, this configuration corresponds to a maximum magnetic field amplitude of 32kA/m on the welding line [54]. One sample is welded for six different welding speeds (0.3, 0.4, 0.5, 0.7, 0.9 and 1.0 mm/s) to be analyzed by optical microscopy, and five, three and three samples are welded for each of the three selected intermediate speeds (0.5, 0.7 and 0.9 mm/s), respectively, to evaluate the mechanical properties of the weld.

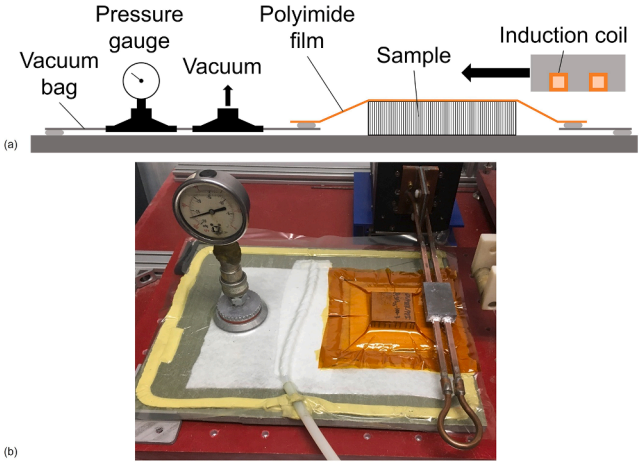

Fig. 3. (a) Schematic and (b) picture of the Vac-IW setup. The black horizontal arrow on the schematic represents the relative movement between the coil and the sample. The speed of the coil displacement corresponds to the welding speed.

3.3. Optical microscopy

One sample from each welding speed is cut as shown on the schematic in Fig. 4 for optical microscopy observation of the weld interface. The samples are mounted into an acrylic mounting compound to be polished and an Olympus GX51 optical microscope is used for the observation.

3.4. Mechanical testing

The skin to core adhesion is characterized using the flatwise tensile (FWT) mechanical test, following the ASTM C297 standard [57]. A steel block is bonded to each side of the sandwich specimen to apply the tensile force evenly on, and normal to, the surface. Loctite® 415™ Super Bonder® instant adhesive is used to bond the steel blocks on the specimens. The parts are stored at room temperature for 24 h to fully cure the

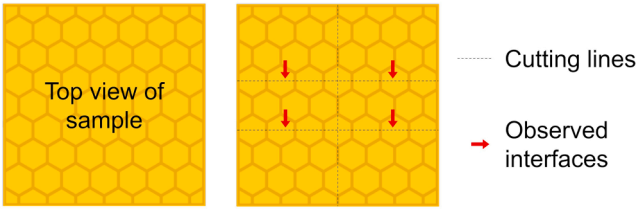

Fig. 4. Schematic of the cutting pattern to extract four optical microscopy samples from a welded sandwich panel.

adhesive.

To execute the FWT mechanical test, an MTS Insight electromechanical tensile testing machine is equipped with the designated jig to hold the sample (manufactured by Wyoming Testing Fixture), as presented in Fig. 5 (right). Specimens with bonded steel blocks are mounted and fixed using pins. The testing speed is 0.5 mm/min, as per the ASTM C297 standard, and a 50 kN load cell is used to record the load during the test.

The main types of possible failures are adhesive (glue) failure (not an acceptable failure mode, leading to an invalid test), facing failure, adhesive failure of the welded joint, cohesive failure of the welded joint or core failure [57]. Hybrid failure, combining at least two acceptable failure modes, can also be reported.

4. Results and discussion

4.1. Optical microscopy

The analysis of the weld interface allows to observe the impact of the process on the contact between the skin and the core. The temperature evolution at the welding line is deduced by observing the deformation of the cell walls. The temperature is not directly monitored by thermocouples due to their inaccuracy in presence of a magnetic field. The first observation is made on samples welded at welding speeds of 0.3 and 0.4 mm/s. At these low speeds, with the applied magnetic field amplitude, too much heat is generated, thereby inducing deformation of the structure, especially towards the center of the structure, as visible in Fig. 6. This sample was welded at 0.3 mm/s. The wall on the left corresponds to the external wall of the sandwich structure. The top of the honeycomb walls is largely deformed (dashed white arrows in Fig. 6), confirming the high temperature experienced in that area. The difference of deformation observed between the edge (black arrow in Fig. 6) and the center is most probably due to a difference in thermal history. There was less heating on the edge due to larger thermal losses on the side of the sandwich structure. The dimensional stability of the sample is not conserved at such low welding speeds. Finally, it also appears that overheating induced a large expansion of porosities in the 3D-printed honeycomb and in the susceptor close to the interface, which might reduce the mechanical properties.

On the other hand, at a welding speed of 1.0 mm/s, the skin is not assembled to the core at all. The parts merely stuck together, and detached shortly after welding, probably due to the induced stress caused by the difference of thermal expansion and contraction of the core and the skin. This indicates that 1.0 mm/s is too fast a welding speed for this combination of materials and applied magnetic field amplitude. This observation on the impact of the welding speed corresponds to what has been reported in the literature [56]. It can be explained by the fact that, at lower speeds, the susceptor is exposed to the magnetic field for a longer duration, which makes it reach higher temperatures, as it was reported by the authors in a previous study [54].

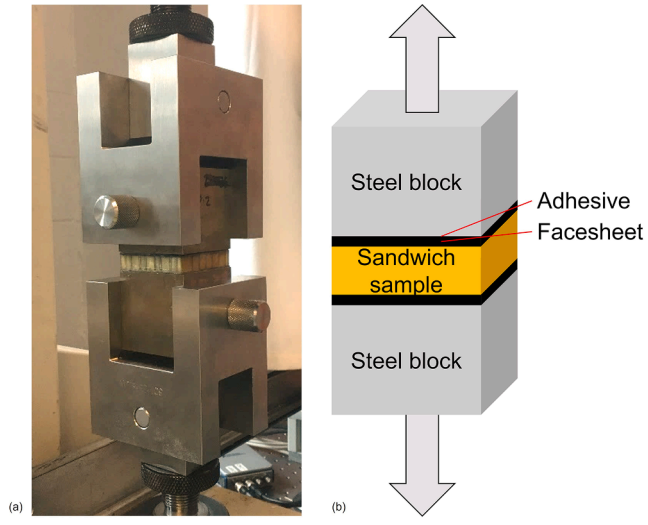

Fig. 5. (a) FWT testing jig installed on the tensile test machine, with a sample mounted to be tested and (b) schematic of the FWT test.

Cross section profile of samples welded at intermediate welding speeds of 0.5, 0.7 and 0.9 mm/s do not exhibit evidence of core crushing, a sign that overheating was avoided (Fig. 7). A good contact seems to have been reached between the skin and the core. The three pictures show an evolution of the contact between the susceptor and the skin. The susceptor final thickness also evolves with the welding speed. The core wall flow observed here is in agreement with reports from the literature, in the context of compression moulding [16]. Here, as the weld is conducted in the upper part of the sandwich structure, the softened core polymer is pulled down by gravity, creating a visible mushroom shape. It appears that welding the sandwich panel upside down could be an alternative, as it would keep the susceptor in contact with the skin. At lower speed (0.5 mm/s, Fig. 7a), a larger susceptor deformation is seen, increasing the contact width with the skin (dashed black lines in Fig. 7). Conversely, at 0.9 mm/s (Fig. 7c), the contact width is smaller and the final susceptor thickness between the skin and the core is larger. These two parameters were measured for each welding speed based on the optical microscopy images; the results are presented in Fig. 8.

4.2. Skin-core interfacial strength

It appears from the optical microscopy observations that the welding speeds of 0.5, 0.7 and 0.9 mm/s correspond to the optimal processing window for this combination of materials (thermoplastic polymer and magnetic particles, under the applied magnetic field amplitude) in this experimental setup. The mechanical properties of the sandwich panels welded at these three speeds are characterized by FWT and presented in Fig. 9. As per the ASTM C297 standard, the strength is expressed as the load at failure divided by the total surface of the sample. For reference, a strength of 6 MPa corresponds to a force of 15 kN. One of the five samples welded at 0.5 mm/s failed inside the core at a lower stress, probably indicating a defect in the honeycomb core created during 3D-printing. This sample is not reported in Fig. 9, as the value does not represent the skin-core strength. Another one failed in the bonding adhesive used to bond the sample to the steel blocks. The maximum load recorded is therefore slightly inferior to the other samples. This value is reported but it should be kept in mind that the actual joint strength is superior to that value. This point is shown in Fig. 9 with a black arrow pointing up. As expected, samples welded at lower speeds exhibit higher strength, as they reached a higher temperature for a longer period of time during the induction welding process. The samples welded at 0.9 mm/s exhibit a lower strength, highlighting the lower quality of the weld at this welding speed. Results of flatwise tensile tests on polymer honeycomb sandwich panels are limited in the literature to compare with the presented values. Grünewald at al. tested PEI foam cores joined to CF/PEEK skins by thermoplastic thermal welding and reported maximum skin-core strength of 1.2 MPa [58]. However, this value corresponds to the foam core failure, which does not indicate the skin-core strength. Another interesting study from Widagdo et al. presents carbon fibre epoxy skins joined to fibre glass honeycomb cores using an epoxy film adhesive [59]. This is not directly comparable as the joining method is not thermoplastic welding but adhesive bonding, but the same mechanical test is used to characterize the samples. Skin-core strengths (cohesive failure inside the adhesive layer) between 5.1 and 5.6 MPa are reported. The results presented here for sandwich samples welded with the Vac-IW method reach up to 6 MPa, without any specific surface preparation. This highlights the good quality of the process.

The samples failure mode is analyzed. One representative sample for

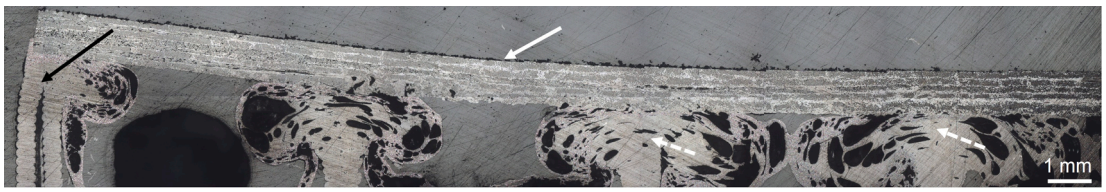

Fig. 6. Cross section profile of a sandwich structure welded at 0.3 mm/s. Left side of the sample corresponds to the outer wall of the sandwich structure (black arrow). Visible deformation is seen on the top skin (solid white arrow). Top of honeycomb cell walls is deformed (dashed white arrows).

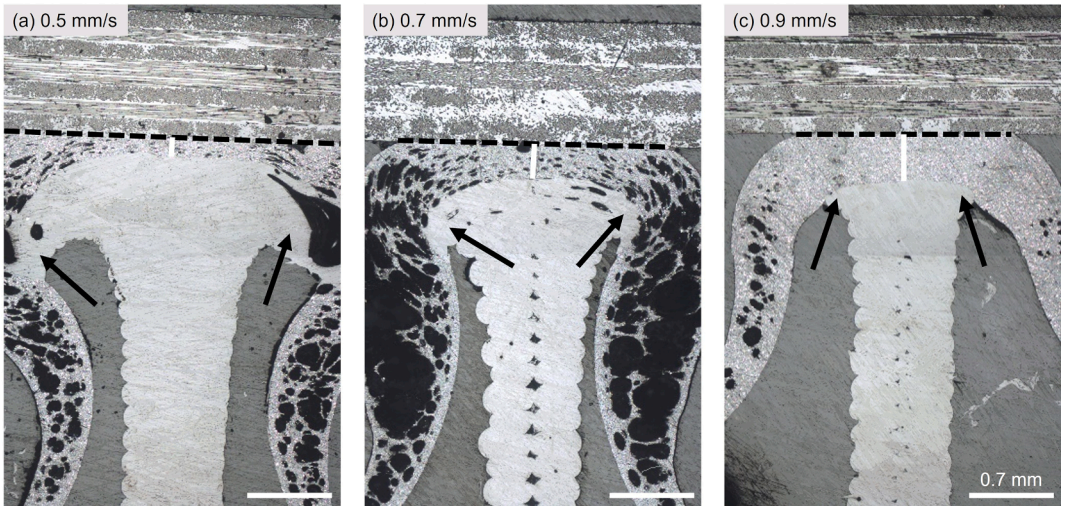

Fig. 7. Welding profile on top of a core cell wall for a sandwich panel welded at (a) 0.5 mm/s, (b) 0.7 mm/s and (c) 0.9 mm/s. Dashed black lines correspond to the contact width. White vertical lines correspond to the susceptor thickness. The deformation of the top of the honeycomb cell walls is highlighted by the black arrows. The white scale bar represents 0.7 mm in the three pictures.

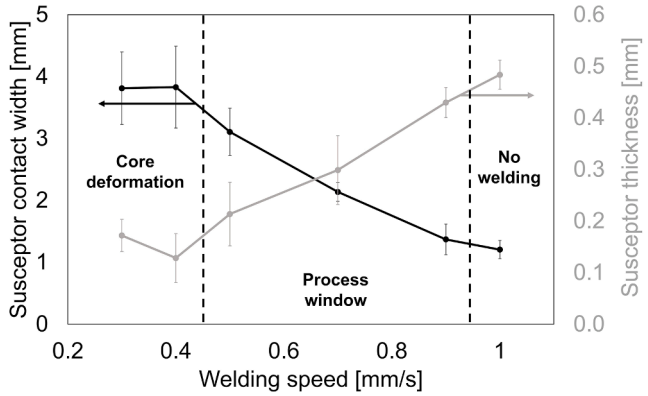

Fig. 8. Susceptor contact width and thickness after welding at different welding speeds.

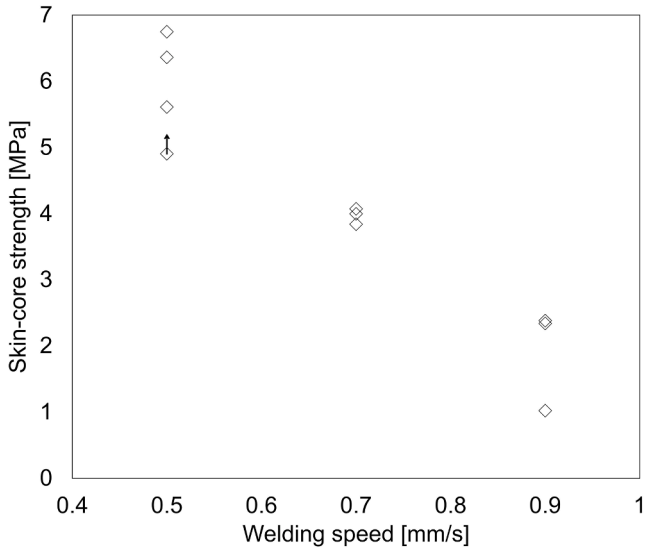

Fig. 9. FWT skin-core strength of welded sandwich samples as a function of the welding speed. Three valid measurements were obtained at each speed. One supplementary sample welded at 0.5 mm/s that broke in the bonding adhesive used to bond the sample to the steel blocks. This value is reported and marked with an arrow pointing up.

each welding speed is presented in Fig. 10. At a welding speed of 0.5 mm/s, the dominant failure mode is a cohesive failure of the susceptor layer, easily identified with its black color (Fig. 10a). At 0.7 mm/s, an adhesive failure is observed either between the skin-susceptor interface or the susceptor/core interface (Fig. 10b). Finally, at 0.9 mm/s, adhesive failure dominates on the whole surface, and is located at the susceptor/core interface (Fig. 10c).

The change in failure mode indicates that the decrease in speed induces a higher degree of welding, caused by a higher temperature reached during the process. The increase of contact width between the core and the skins observed in the optical microscopy images is confirmed by the change of failure behaviour observed in the fractured samples. This has been previously reported in the literature [60]. The effective contact surface area is increased at a low welding speed, which contributes to the improvement of the mechanical strength. In the three specimens, welding was less advanced close to the edges of the skin. This is especially visible on the sample welded at 0.5 mm/s (Fig. 10 top picture). As discussed, the dominant failure mechanism in this case is

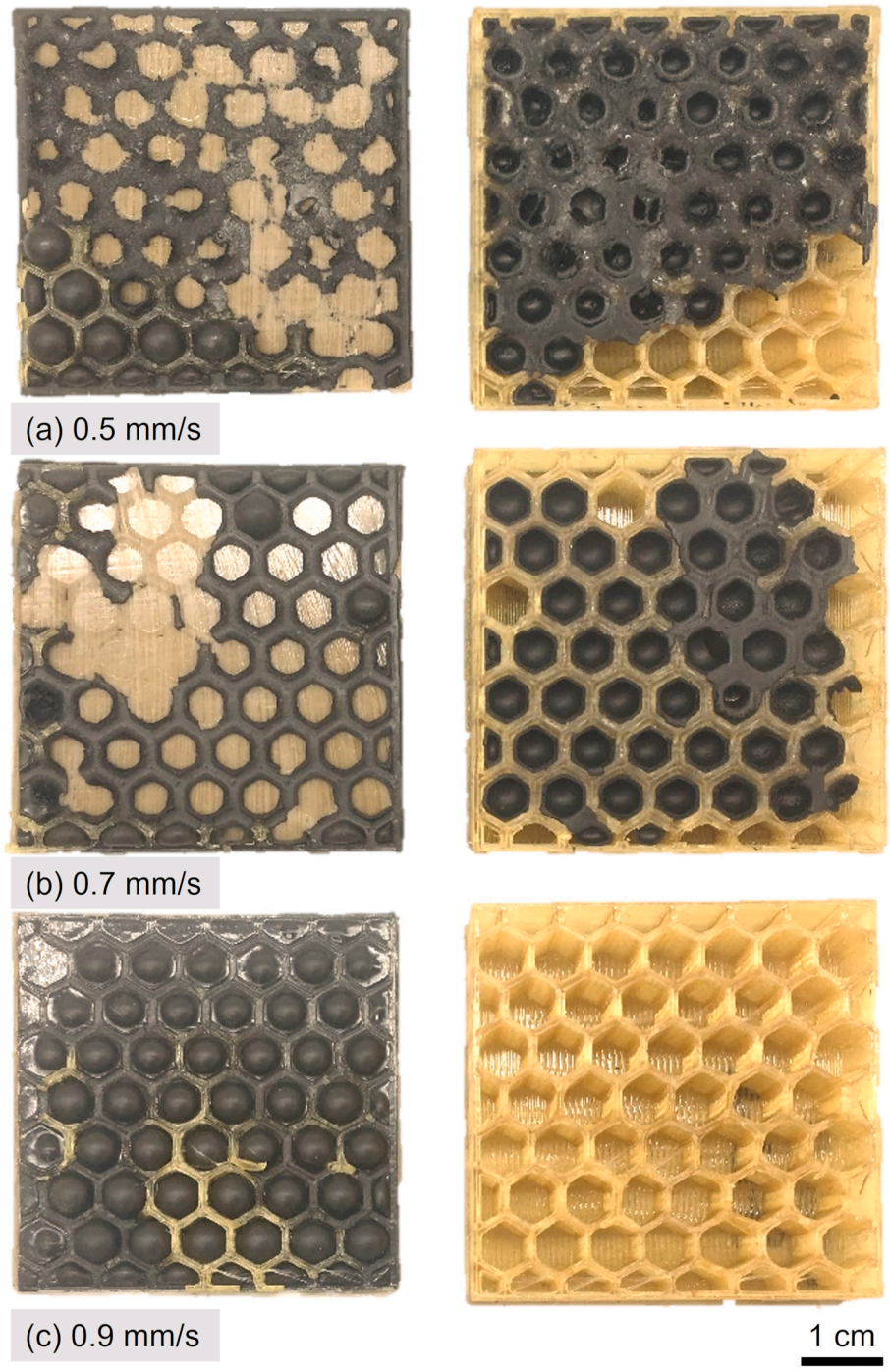

Fig. 10. Fractured FWT sandwich samples welded at (a) 0.5 mm/s, (b) 0.7 mm/s, (c) 0.9 mm/s).

cohesive failure, but on top of the outside wall, the failure is clearly adhesive, highlighting the lower degree of welding in that region.

4.3. Effective skin-core strength

The fracture analysis shows a higher degree of welding in the samples welded at low speeds. Another way to verify this is to normalize the strength of the skin to core interface by the effective surface area of contact between the skin and the core. As mentioned above and reported in Fig. 8, the susceptor contact width with the skin increases when the welding speed decreases, as observed in the optical microscopy images. By assuming that this effective contact width is constant throughout the structure, it is possible to calculate the effective contact surface area, as shown in Fig. 11. For example, as highlighted by the dashed lines in Fig. 11, the effective contact surface area evolves from 25 % with the original 0.8 mm wall thickness to 60 % with 2.4 mm wall thickness. The effective contact surface area is more than doubled, which in turn impacts the skin-core strength of the sandwich panel. Based on this assumption, it is possible to calculate the effective interfacial strength by dividing the load at failure by the effective contact surface area instead of the skin surface area. These results are presented in Fig. 12. If the increase in strength observed in Fig. 9 was only caused by the larger contact surface area, then the data points in Fig. 12 would all be aligned. As it appears, the normalized strength of the sandwich sample increases

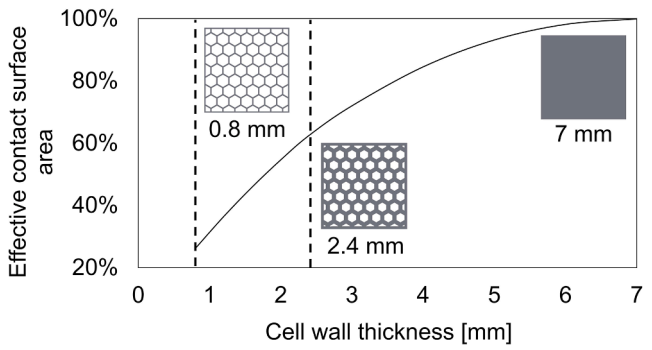

Fig. 11. Effective contact surface area of a honeycomb core as a function of the cell wall thickness. The two dashed lines highlight the original 0.8 mm and the 2.4 mm wall thicknesses.

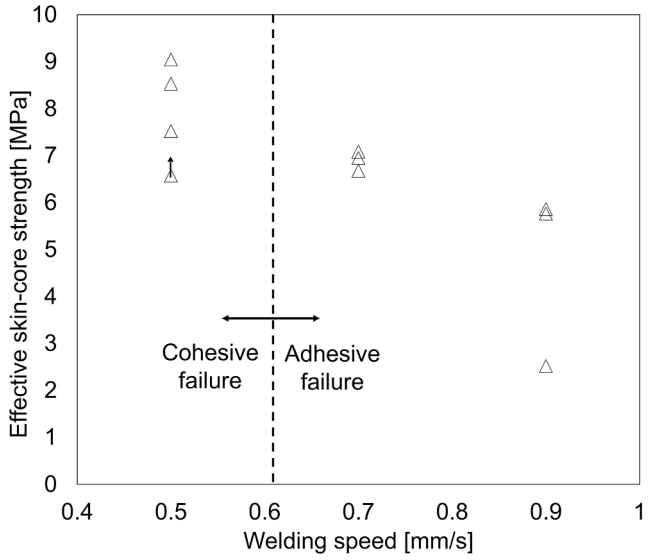

Fig. 12. Effective skin-core interfacial strength as a function of the welding speed. Three valid measurements were obtained at each speed. One supplementary sample welded at 0.5 mm/s that broke in the bonding adhesive used to bond the sample to the steel blocks. This value is reported and marked with an arrow pointing up. The dominant failure mode is indicated.

when the welding speed is reduced, which further confirms that a higher degree of welding is achieved at lower speeds, which can be related to the observations on the fractured samples (Fig. 10).

5. Conclusion

This paper presents a new method for joining thermoplastic composites sandwich structures under vacuum and using induction welding. The described Vac-IW method proposes a contactless induction welding method, allowing for heat localisation at the joining interface with a constant pressure application during the process. The atmospheric pressure applied during assembly, which is usually considered too low to weld or consolidate high performance thermoplastics, is shown to be high enough here, due to the effective higher pressure supported by the core cell walls. The optical microscopy observations allowed to define an appropriate processing window and the FWT mechanical tests validated that welding occurred between the skin and the core, proving the feasibility of the technique. The application of the dual-polymer bonding method on the sandwich skins allows for the weld to occur at a lower temperature than the skin thermoplastic matrix melting point, avoiding issues like deconsolidation. Although it is tested with a honeycomb core in this study, the Vac-IW method can also be applied to corrugated or foam cores made of thermoplastic polymers. This study demonstrates the feasibility of the method, which is promising for the assembly of thermoplastic composite sandwich structures, without having to heat non-electrically-conductive skins through their thickness. The contactless approach showed here may also open the door to the assembly of non-flat thermoplastic composite sandwich panels on which a coil could be moved using a robot with temperature control through the susceptor Curie temperature and thermabond process. In the future, thermoplastic sandwich panels assembled with the Vac-IW method should be tested in 3-points bending and double cantilever beam test, to assess the fracture toughness of the weld and compare with other experiments reported in the literature.

CRediT authorship contribution statement

R.G. Martin: Writing – original draft, Visualization, Methodology, Investigation, Conceptualization. **C. Johansson:** Writing – review & editing, Supervision. **J.R. Tavares:** Writing – review & editing, Supervision. **M. Dubé:** Writing – review & editing, Supervision.

Declaration of competing interest

The authors declare that they have no known competing financial interests or personal relationships that could have appeared to influence the work reported in this paper.

Data availability

Data will be made available on request.

Acknowledgements

The authors acknowledge financial support from CREPEC (Research Center for High Performance Polymer and Composite Systems), NSERC (Natural Sciences and Engineering Research Council of Canada) (grant number ALLRP 556497-20), PRIMA Québec (Pôle de Recherche et d'Innovation en Matériaux Avancés) (grant number R20-13-004), the Canadian Space Agency (CSA), Ariane Group, NanoXplore inc, Mekanik and Dyze Design. They also want to thank Mr. Adrien Fage (Ariane Group) for his help with the optical microscopy images, as well as Mr. Kambiz Chizari and Mr. Olivier Duchesne (Polytechnique Montréal) for their help with the mechanical tests.

References

[1] Williamson JR. Advanced materials for space structures. Acta Astronaut 1991;24:197–202.
[2] Daniel I, Gdoutos E. Failure modes of composite sandwich beams. Major Accomplishments in Composite Materials and Sandwich Structures: An Anthology of ONR Sponsored Research 2010:197–227.
[3] T. Neumeyer, J. F. Knoechel, M. Mühlbacher, T. Kroeger, V. Altstädt, P. Schreier. Thermoplastic Sandwich Structures - Processing Approaches Towards Automotive Serial Production. In: Proceedings of 21st International Conference on Composite Materials. Xi'an, China, 2017.
[4] Gao X, Zhang M, Huang Y, Sang L, Hou W. Experimental and numerical investigation of thermoplastic honeycomb sandwich structures under bending loading. Thin-Walled Struct 2020;155:106961.
[5] Skawinski O, Binetruy C, Krawczak P, Grando J, Bonneau E. All-Thermoplastic composite sandwich panels – part I: manufacturing and improvement of surface quality. J Sandw Struct Mater 2004;6(5):399–421.
[6] B. Vieille, V. M. Casado, C. Bouvet. Comparative study on the impact behavior and damage tolerance of woven carbon fiber reinforced thermoplastic– and thermosetting– composites. In: Proceedings of ECCM15 - 15th European conference on composite materials. Venice, Italy, 2012, p. 1-8.
[7] Grünewald J, Parlevliet P, Altstädt V. Manufacturing of thermoplastic composite sandwich structures: a review of literature. J Thermoplast Compos Mater 2017;30(4):437–64.
[8] Pegoretti A. Towards sustainable structural composites: a review on the recycling of continuous-fiber-reinforced thermoplastics. Advanced Industrial and Engineering Polymer Research 2021.
[9] Kodiyalam S, Nagendra S, DeStefano J. Composite sandwich structure optimization with application to satellite components. AIAA J 1996;34(3):614–21.

[10] Gao X, Zhang M, Huang Y, Sang L, Hou W. Experimental and numerical investigation of thermoplastic honeycomb sandwich structures under bending loading. Thin-Walled Struct 2020;155.
[11] Özen I, Cava K, Gedikli H, Alver Ü, Aslan M. Low-energy impact response of composite sandwich panels with thermoplastic honeycomb and reentrant cores. Thin-Walled Struct 2020;156.
[12] Townsend S, Adams R, Robinson M, Hanna B, Theobald P. 3D printed origami honeycombs with tailored out-of-plane energy absorption behavior. Mater Des 2020;195.
[13] Walter NA, Scialdone JJ. Outgassing Data for Selecting Spacecraft Materials 1997.
[14] Grünewald J. Thermoplastic composite sandwiches for structural helicopter applications. Germany: University of Bayreuth; 2018. Ph.D. Thesis.
[15] B. T. Åström, M. Akermo, A. Carlsson, L. D. McGarva. All-thermoplastic sandwich concept. In: Proceedings of Sandwich Construction 4: Fourth International Conference on Sandwich Construction. Stockholm, Sweden, 1998, p. 705-718.
[16] Åkermo M, Aström BT. Modeling compression molding of all-thermoplastic honeycomb core sandwich components. Part A: Model development *Polym Compos* 2000;21(2):245–56.
[17] Breuer U, Ostgathe M, Neitzel M. Manufacturing of all-thermoplastic sandwich systems by a one-step forming technique. Polym Compos 1998;19(3):275–9.
[18] K. A. Brown, R. Brooks, N. A. Warrior, P. P. Kulandaivel. Modelling the impact behaviour of thermoplastic composite sandwich structures. In: Proceedings of 16th International Conference on Composite Materials ICCM-16. Kyoto, Japan, 2007.
[19] Denkena B, Schmidt C, Schmitt C, Kaczemirzk M. Experimental investigation on the use of a PEI foam as core material for the in-situ production of thermoplastic sandwich structures using laser-based thermoplastic automated fiber placement. Materials 2022;15(20).
[20] Wingfield JRJ. Treatment of composite surfaces for adhesive bonding. Int J Adhes Adhes 1993;13(3):151–6.
[21] Ageorges C, Ye L, Hou M. Advances in fusion bonding techniques for joining thermoplastic matrix composites: A review. Compos A Appl Sci Manuf 2001;32:839–57.
[22] Yousefpour A, Hojjati M, Immarigeon J-P. Fusion bonding/welding of thermoplastic composites. J Thermoplast Compos Mater 2004;17(4):303–41.
[23] Grünewald J, Parlevliet P, Altstädt V. Definition of process parameters for manufacturing of thermoplastic composite sandwiches – part B: model verification. J Thermoplast Compos Mater 2018;31(6):803–19.
[24] R. Brooks, P. Kulandaivel, C. Rudd. Skin Consolidation in Vacuum Moulded Thermoplastic Composite Sandwich Beams. In: Proceedings of 8th International Conference on Sandwich Structures ICSS8. Porto, Portugal, 2008, p. 627-637.
[25] Rozant O, Bourban P-E, Månson J-A-E. Manufacturing of three-dimensional sandwich parts by direct thermoforming. Compos A Appl Sci Manuf 2001;32(11):1593–601.
[26] Grünewald J, Parlevliet P, Altstädt V. Definition of process parameters for manufacturing of thermoplastic composite sandwiches – part A: modelling. J Thermoplast Compos Mater 2017.
[27] T. Latsuzbaya, P. Middendorf, D. Voelkle, C. Weber. Fusion Bonding of Thermoplastic Mono-material Sandwich Structures with Honeycomb Core. In: Proceedings of SAMPE International Conference 2023, Seattle, WA, USA, 2023.
[28] Trende A, Åström BT, Wöginger A, Mayer C, Neitzel M. Modelling of heat transfer in thermoplastic composites manufacturing: double-belt press lamination. Compos Part Appl Sci Manuf 1999;30(8):935–43.
[29] Xinyu F, Yubin L, Juan L, Chun Y, Ke L. Modeling of heat conduction in thermoplastic honeycomb core/face sheet fusion bonding. Chin J Aeronaut 2009;22(6):685–90.
[30] Ahmed TJ, Stavrov D, Bersee HEN, Beukers A. Induction welding of thermoplastic composites—an overview. Compos A Appl Sci Manuf 2006;37(10):1638–51.
[31] Brassard D, Dubé M, Tavares JR. Resistance welding of thermoplastic composites with a nanocomposite heating element. Compos B Eng 2019;165:779–84.
[32] Brassard D, Dubé M, Tavares JR. Modelling resistance welding of thermoplastic composites with a nanocomposite heating element. J Compos Mater 2021;55(5):625–39.
[33] Bayerl T, Duhovic M, Mitschang P, Bhattacharyya D. The heating of polymer composites by electromagnetic induction – a review. Compos A Appl Sci Manuf 2014;57:27–40.
[34] Dubé M, Hubert P, Yousefpour A, Denault J. Current leakage prevention in resistance welding of carbon fibre reinforced thermoplastics. Compos Sci Technol 2008;68(6):1579–87.
[35] Rudolf R, Mitschang P, Neitzel M. Induction heating of continuous carbon-fibre-reinforced thermoplastics. Compos A Appl Sci Manuf 2000;31:1191–202.
[36] Mitschang I, Rudolf R, Neitzel M. Continuous induction welding process, modelling and realisation. J Thermoplast Compos Mater 2002;15:127–53.
[37] Pappadà S, Salomi A, Montanaro J, Passaro A, Caruso A, Maffezzoli A. Fabrication of a thermoplastic matrix composite stiffened panel by induction welding. Aerosp Sci Technol 2015;43:314–20.
[38] Fink BK, McCullough RL, Gillespie JJW. A local theory of heating in cross-ply carbon fiber thermoplastic composites by magnetic induction. Polym Eng Sci 1992;32(5):357–69.
[39] Barazanchy D, van Tooren M. Heating mechanisms in induction welding of thermoplastic composites. J Thermoplast Compos Mater 2023;36(2):473–92.
[40] C. Worrall, R. Wise. Novel Induction Heating Technique for Joining of Carbon Fibre Composites. In: Proceedings of *ECCM16*. Sevilla, Spain, 2014.
[41] Yarlagadda S, Fink BK, Gillespie JJW. Resistive susceptor design for uniform heating during induction bonding of composites. J Thermoplast Compos Mater 2016.
[42] Dermanaki Farahani R, Janier M, Dubé M. Conductive films of silver nanoparticles as novel susceptors for induction welding of thermoplastic composites. Nanotechnology 2018;29.
[43] Dermanaki Farahani R, Dubé M. Novel heating elements for induction welding of carbon fiber/polyphenylene sulfide thermoplastic composites. Adv Eng Mater 2017;19(1).
[44] Suwanwatana W, Yarlagadda S, Gillespie JJW. Hysteresis heating-based induction bonding of thermoplastic composites. Compos Sci Technol 2006;66(11):1713–23.
[45] Bae D. Heating behavior of ferromagnetic Fe particle-embedded thermoplastic polyurethane adhesive film by induction heating. J Ind Eng Chem 2015;30:92–7.
[46] Bayerl T, Schledjewski R, Mitschang P. Induction Heating of Thermoplastic Materials by Particulate Heating Promoters. Polym Compos 2012;20:333–42.
[47] Wetzel ED, Fink BK. Feasibility of Magnetic Particle Films for Curie Temperature-Controlled Processing of. Composite Materials 2001.
[48] Martin RG, Johansson C, Tavares JR, Dubé M. Material selection methodology for an induction welding magnetic susceptor based on hysteresis losses. Adv Eng Mater 2022;24(3).
[49] Coey JMD. Magnetism and Magnetic Materials. Cambridge University Press; 2010.
[50] F. N. Cogswell, P. J. Meakin, A. J. Smiley, M. T. Harvey, C. Booth. Thermoplastic interlayer bonding of aromatic polymer composites. *Composites Manufacturing*, p. 2315-2325, Reno, NV, USA, 1989.
[51] Smiley A, Halbritter A, Cogswell F, Meakin PJ. Dual polymer bonding of thermoplastic composite structures. Polym Eng Sci 1989;31(7):526–32.
[52] Meakin PJ, Cogswell FN, Halbritter AJ, Smiley AJ, Staniland PA. Thermoplastic interlayer bonding of aromatic polymer composites—methods for using semi-crystallized polymers. Compos Manuf 1991;2(2):86–91.
[53] SABIC. ULTEM Resin 1010 Technical data sheet. 2021.
[54] R. G. Martin, M. Figueiredo, C. Johansson, J. R. Tavares, M. Dubé. Hysteresis Losses Magnetic Susceptor Heating Rate Characterization. In: Proceedings of SAMPE 2023 conference. Seattle, WA, USA, 2023, p. 1112-1127.
[55] Bastien LJ, Gillespie JW. A non-isothermal healing model for strength and toughness of fusion bonded joints of amorphous thermoplastics. Polym Eng Sci 1991;31(24):1720–30.
[56] F. Lionetto, S. Pappadà, G. Buccoliero, A. Maffezzoli, Finite element modeling of continuous induction welding of thermoplastic matrix composites, *Materials and Design*, vol. 120, p. 212-221.
[57] ASTM, ASTM C297 Standard Test Method for Flatwise Tensile Strength of Sandwich Constructions. 2021.
[58] Grünewald J, Parlevliet PP, Matchinski A, Altstädt V. Mechanical performance of CF/PEEK–PEI foam core sandwich structures. J Sandw Struct Mater 2019;21(2):2680–99.
[59] Widagdo D, Kuswoyo A, Nurpratama TO, Hadi BK. Experimental flatwise tensile strength dataset of carbon fibre reinforced plastic sandwich panels with different core material preparations. Data Brief 2020;28.
[60] Åkermo M, Aström BT. Modeling compression molding of all-thermoplastic honeycomb core sandwich components – Part B: Model verification. Polym Compos 2000;21(2):257–67.